Combust. Sci. and Tech., 182: 215–230, 2010

ISSN: 0010-2202 print/1563-521X online
DOI: 10.1080/00102200903341538

Taylor & Francis
Taylor & Francis Group

FINE FUEL HEATING BY RADIANT FLUX

David Frankman,[1] Brent W. Webb,[1] Bret W. Butler,[2] and Don J. Latham[2]

[1]*Department of Mechanical Engineering, Brigham Young University, Provo, Utah, USA*

[2]*Rocky Mountain Research Station, U.S. Forest Service Fire Sciences Laboratory, Missoula, Montana, USA*

Experiments were conducted wherein wood shavings and Ponderosa pine needles in quiescent air were subjected to a steady radiation heat flux from a planar ceramic burner. The internal temperature of these particles was measured using fine diameter (0.076 mm diameter) type K thermocouples. A narrow angle radiometer was used to determine the emissive power generated by the burner. A model was developed to predict the steady-state temperature of a cylindrical particle with an imposed radiation heat flux under both quiescent air (buoyancy-induced cooling) and windy (forced convection cooling) conditions. Excellent agreement was observed between the model predictions and the experimental data. Parametric studies using the validated model explore the effect of burner (flame) temperature and distance, fuel size, and wind speed. The data suggest that ignition of the fuel element by radiation heating alone is likely only under circumstances where the fire is very intense (such as crown fires), and even then may still be dependent on pilot ignition sources.

Keywords: Fine fuel; Heating; Radiation

INTRODUCTION

Radiation and convection heat transfer have complimentary roles in wildland fire spread (Anderson, 1969), but due to the complexity of the wildland fire environment, they remain largely undetermined. Previous work (Anderson, 1969; Asensio & Ferragut, 2002; Catchpole et al., 1998) suggests that—especially in the case of crown fires—intense radiative transfer from the flame pre-heats fuel ahead of the flame front, while convection transfer brings hot combustion products into intimate contact with fuel particles. Others conclude that radiation dominates fuel preheating (Albini, 1985; Telisin, 1973). It is most likely that the relative contributions of these two heat transfer modes to fuel preheating and fire spread depend in a complex way on the local environment and fuel properties. Clearly, the balance between radiation and convection is not well understood. A detailed understanding of the relative

Received 9 February 2009; revised 4 September 2009; accepted 16 September 2009.
Address correspondence to Brent W. Webb, Department of Mechanical Engineering, Brigham Young University, Provo, UT 84602. E-mail: webb@byu.edu

contributions of radiative and convective transfer in wildland fires is critical to the understanding of the wildland fire ignition, spread, and intensity. It is evident that both modes of heat transfer participate in crown, ground, and surface fire spread. This work seeks to add insight to this question.

Significant effort has been directed at understanding the heating and ignition of solid wood blocks (Simms, 1963), but only a few studies have explored the contributions of radiative and convective heat transfer in widland fire phenomena. Van Wagner (1967) concluded that radiation is the dominant preheating mechanism in the fuel ignition process through a series of pine needle bed fire spread experiments. A subsequent study defined temperature thresholds above which cellulosic materials would ignite (Anderson, 1969). Anderson conducted experiments in which it was determined that radiation contributed no more than 40% of the energy required for ignition. Pagni (1972) conducted a series of experiments demonstrating that under no-wind ambient conditions, radiation was dominant, but in wind-aided flame spread, convection was dominant. Telisin (1973) developed a radiation-driven fire model that included an extinction distance equal to the mean free path within the fuel. This model did not agree well with experimental results reported. Hirano and Sato (1974) showed in an experimental study of combusting paper that hot gases existed only very near the flame. The pine needle litter experiment of Konev and Sukhinin (1977) revealed that a steadily spreading fire contributes approximately 37% of the energy for ignition and 8% for a nearly extinguished flame. Albini (1985) developed a wildland fire model that rigorously solved the governing equation of radiative transfer, neglecting convective transfer completely. The model was subsequently modified to include fuel cooling by natural convection (Albini, 1986). However, the model did not include convective pre-heating of the fuel. Weber (1991) identified radiation heat transfer as the dominant heat transfer mode in forest fires through a simple analytical model, and expressed the need for a short-range heat transfer mechanism for fires in still air. Dupuy (2000) used experiments to verify multiple radiation driven models to determine if radiation alone can describe experimental results when it is considered as the dominant heat transfer mechanism in flame spread. It was concluded that a radiation-dominant model could not account for experimental observations. Butler et al. (2004) report direct measurements of energy transfer in full-scale crown fires. The data suggest that radiative heating can account for the bulk of the particle heating ahead of the flaming front, but that immediately prior to ignition, convective heating is significant and possibly required for ignition.

The survey of literature presented in the preceding paragraphs indicates that there remains considerable uncertainty regarding the relative roles of radiation and convection heat transfer in combustion of wildland fuel. No consistent comprehensive picture has yet emerged regarding the relative contribution of radiant and convective heating to wildland fire ignition, spread, and intensity. This paper presents both experimental and analytical work seeking to explore the pre-heating mechanism of fine fuels in a controlled environment. The experiments and analysis presented here are designed to explore the parameters affecting the radiant heating and convective cooling and heating of fine dead woody fuels. The findings apply primarily to crown fire spread through suspended dead vegetation, but also have application for flaming ground fires spreading through dead plants, needles, and

leaves on or near the surface of the ground, and, to some extent, to the same fire spread in live vegetation. The experiments do not simulate smoldering combustion of litter and duff on the ground surface.

EXPERIMENTS

A series of experiments were conducted in which fine fuel samples were subjected to an imposed radiant heat flux in a quiescent-air environment, and their steady-state temperature recorded as a function of distance from the heat source, as shown schematically in Figure 1. Fuel samples were prepared of two sizes of shavings of aspen (*Populus tremuloides*) termed fine (nominally $0.8\,\text{mm} \times 0.6\,\text{mm}$ cross-section) and large (nominally $2.5\,\text{mm} \times 0.8\,\text{mm}$ cross-section) excelsior, and Ponderosa pine (*Pinus ponderosa*) needles (nominally $1.6\,\text{mm} \times 0.8\,\text{mm} \times 5\,\text{cm}$ long). Neither the excelsior nor the pine needles have a round cross-section. The excelsior has a rectangular cross-section, whereas the Ponderosa pine needle cross-sections have three sides: two flat sides with a subtended angle of 120° and the third side curved. The cross-sectional shape of the Ponderosa pine needles is such that if flat sides are placed adjacent to flat sides, three needles will form a cylindrical fascicle (Wykoff, 2002). Because the cross-section of the fuels used in this experiment was not round, the hydraulic diameter (Munson et al., 2002) was used to characterize the size. The hydraulic diameter of the small and large excelsior and Ponderosa pine fuel samples was measured as 0.44, 1.29, and 0.70 mm, respectively.

Small-bead (0.076 mm diameter wire) type K thermocouples were pressed into the back (non-burner-exposed) surface of the fine and coarse excelsior samples, as shown in the photograph of Figure 2. The thermocouple wires were wound around the fuel sample and connected to larger lead wires connecting the thermocouple to the data acquisition system. It is understood that thermocouple temperature measurements can suffer significant error in combustion systems (Shaddix, 1998). However, in this study, the thermocouples embedded in the fuel particles were

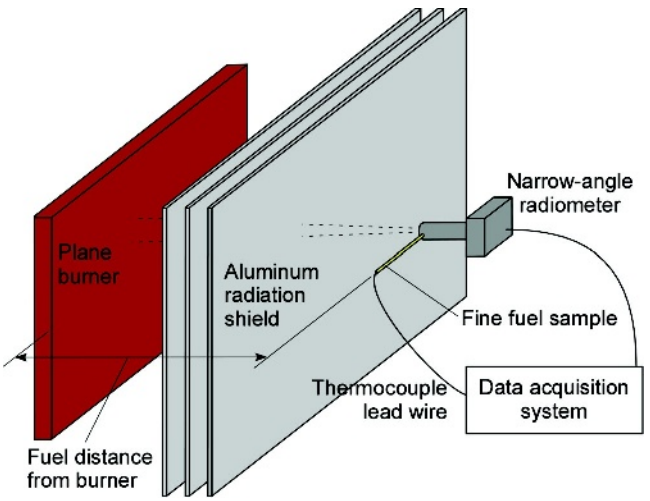

Figure 1 Experimental setup.

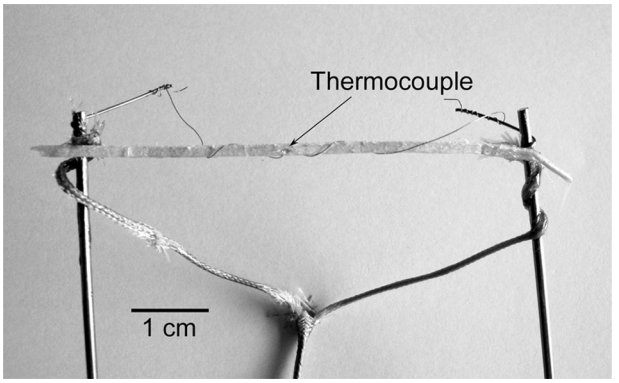

Figure 2 Photograph of thermocouple instrumentation on fine fuel element.

mounted with the bead pressed into the wood surface to enhance direct thermal contact with the wood and to minimize errors due to radiant loss or gain. Assuming that radiation errors are minimal, the fuel surface temperature measurements are estimated to be accurate to within a few degrees. The fuel samples were dried to 6% fuel moisture in a 297 K environment with a 20% relative humidity. A fuel sample of a given composition and size was mounted horizontally with thermocouple lead wires drawn away from the fuel sample. The sample was positioned parallel to and along the centerline of the burner at distances of 0.15, 0.25, 0.35, and 0.45 m from the burner surface. The sample was also positioned horizontally such that any buoyant draft from the particle resulted in a convective cross flow. Thermocouple and narrow

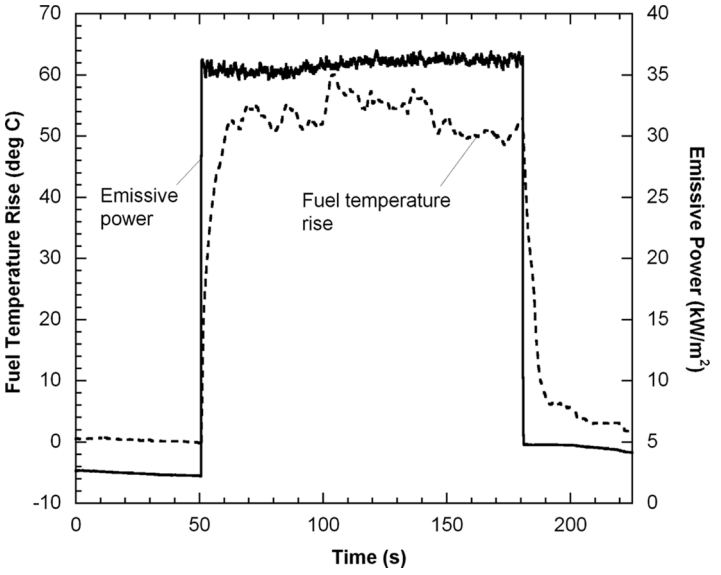

Figure 3 Representative sample of experimentally measured timewise variation in heat flux and fuel temperature rise above ambient.

angle radiometer data were acquired using a multi-channel data acquisition system. As shown schematically in Figure 1, the radiometer was positioned immediately beside the fuel sample such that it could not interfere with the flow of air around the sample.

The experiments were performed in a large room free of drafts from the movement of persons or operation of exhaust fans. The radiant flux was provided by a propane-fired rectangular ceramic plane diffusion burner of dimensions 0.15×0.23 m. The flame forms on the ceramic surface where the propane fuel mixes with atmospheric oxygen. Once the fuel sample with the thermocouples was positioned properly, the burner was lit and allowed to stabilize for 2 to 3 minutes. A radiation

Table 1 Average fuel temperature and emissive power for all experiments

	Distance from burner (cm)	Experimental repetition #	Average fuel temperature (K)	Fuel temperature SD (K)	Emissive power (kW/m^2)	Emissive power SD (kW/m^2)
Small excelsior	15	1	364.4	2.6	39.3	0.8
	15	2	363.4	4.5	40.6	0.7
	15	3	364.3	3.0	38.2	0.8
	25	1	329.5	1.6	37.7	0.8
	25	2	331.0	2.2	38.0	0.4
	25	3	331.4	3.2	37.4	0.4
	35	1	326.0	2.5	34.4	0.7
	35	2	326.0	1.9	34.8	0.4
	35	3	325.1	2.3	34.1	0.4
	45	1	309.6	1.2	35.1	0.6
	45	2	310.5	1.2	35.1	0.5
	45	3	310.3	1.0	34.5	0.4
Large excelsior	15	1	401.5	7.1	37.4	0.6
	15	2	399.5	7.5	37.3	0.9
	15	3	402.1	6.9	36.5	0.8
	25	1	353.8	3.4	35.7	1.5
	25	2	347.9	3.2	35.9	0.5
	25	3	350.9	4.3	35.6	0.5
	35	1	335.5	1.9	32.9	0.4
	35	2	334.9	1.2	32.8	0.5
	35	3	333.6	3.3	33.3	0.6
	45	1	322.5	1.3	33.2	0.3
	45	2	323.5	1.8	33.0	0.3
	45	3	323.5	2.7	32.8	0.7
Ponderosa pine	15	1	390.9	1.9	38.3	0.9
	15	2	390.5	2.8	37.8	0.7
	15	3	390.4	1.7	37.1	0.9
	25	1	349.3	4.1	36.6	0.5
	25	2	351.7	4.6	36.2	0.5
	25	3	351.0	2.6	35.9	0.8
	35	1	328.6	1.1	33.4	0.5
	35	2	329.2	2.6	33.3	0.3
	35	3	330.4	2.3	33.1	0.5
	45	1	318.3	1.1	34.2	0.5
	45	2	319.3	1.4	34.6	0.3
	45	3	320.6	1.4	34.0	0.3

shield (consisting of three 30 cm × 30 cm square aluminum sheets separated by 2 cm each) between the fuel and burner was then quickly removed, exposing the fuel to the radiation from the burner. Temperature data from the thermocouple was sampled at a rate of 10 Hz. A narrow angle radiometer described elsewhere (Butler, 1993) was positioned beside the fuel, and the local emissive power was measured. Based on repeated measurements and exploration of the variation across the burner surface, the reported measurement was assumed to be representative of the entire burner surface, and was used to determine the radiant heat flux emitted by the ceramic plane burner and incident on the fuel samples. The emissive power data were collected simultaneous to the temperature data. The collection angle of the radiometer was 4.5°, and its measurement accuracy is estimated to be within 3% (Butler, 1993). Figure 3 illustrates a representative history of fuel temperature rise above ambient temperature and irradiation shown for a Ponderosa pine needle sample at a 25 cm distance from the burner. After a short transient, the irradiation and temperature reach a nominally steady value, with fluctuations in temperature never exceeding 7 K maximum-to-minimum, and the irradiation fluctuations were confined to 1–1.5 kW/m^2. Measurements for each fuel type at the four burner-fuel separation distances were repeated three times. The temporal fuel temperature and irradiation data were averaged over the typical 2–2.5-minute sample period. The averaged absolute fuel temperature and standard deviations are included in Table 1 for all experiments. The data show that the fluctuations in measured temperature are quite small, but generally increase closer to the ceramic burner.

Figure 4 shows the experimentally measured average fuel temperature rise above ambient as a function of distance for the three fuels investigated. Multiple

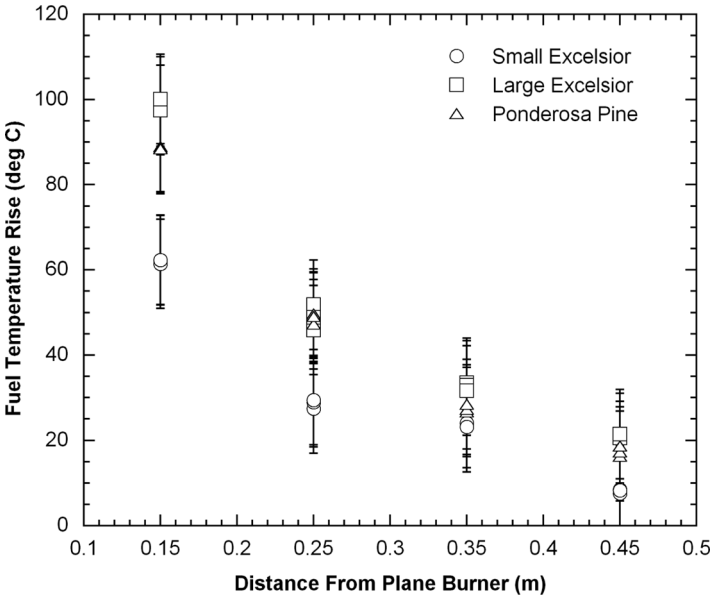

Figure 4 Experimentally measured fuel temperature rise above ambient as a function of distance from plane burner for Ponderosa pine and small and large excelsior.

tests at the same experimental conditions and location relative to the burner are shown as separate data points, and reveal the data to be very repeatable. The data show that, as expected, the highest fuel temperatures are experienced by samples near the burner, with temperatures reaching 400 K for the large excelsior fuel samples at a distance of 0.15 m from the burner plane. Fuel temperature is seen to decrease with increasing distance from the burner. At 0.45 m from the burner plane, the fuel temperatures are nominally at or below 320 K. Smaller fuel results in lower temperatures at a given separation distance, as seen by comparing the large and small excelsior samples. This is due to the smaller capture area for radiative transfer incident on the fuel sample. The Ponderosa pine samples exhibit temperatures that lie generally between the two excelsior sample sizes at all separation distances.

MODEL

A mathematical model of the energy transfer for an individual fuel particle was developed. The model assumed a small fuel element of cylindrical cross-section with known diameter suspended in air. The fuel particle is heated by exposure to irradiation from a radiatively black heat source of finite size and known temperature T_b, and is cooled by convective and radiative loss to the ambient air and surroundings at temperature $T_\infty = 293$ K. The particle is located at a specified distance from the burner surface and is allowed to reach a steady-state temperature. It should be mentioned that energy transfer to the particle through convection once the fuel element enters the natural convection boundary layer at the front of the rectangular plane burner is possible. The thickness of the boundary layer was evaluated using the similarity solution of Ostrach (1953) for the free convection boundary layer on a vertical heated rectangular plane. The analysis indicated that the thickness of the boundary layer along the burner plane was approximately 0.03 m. Therefore, the boundary layer at the front of the ceramic planar burner was not considered in the model. It should be further mentioned that desiccation and devolatilization were not considered in the model. As mentioned previously, the fuel samples used in the experimental work were dried prior to testing. The range of temperatures at which devolatilization occurs is found in the literature. Susott (1980) showed that volatiles generation begins at a temperature of 463 K (190°C), with maximum mass release at 623 K (350°C) in Ponderosa pine needles. Stamm (1964) suggests that thermal degradation of solid wood samples occurs at temperatures as low as 498 K, but that substantial degradation does not occur until 523 K. Clearly, ignition temperature is dependent on the rate of heating, sample dimensions and morphology, presence or absence of volatile compounds, presence of moisture, and other factors (Drysdale, 1985; Stamm, 1964). Consequently, a fixed ignition temperature has relatively little meaning. However, for the purposes of this discussion, 523 K has been selected as a representative minimum ignition temperature for the fine dead woody samples used in this study. This temperature matches the minimum ignition temperature indicated by Babrauskas (2003). Others have selected ignition temperatures in this range (Catchpole et al., 1998; Pagni, 1972; Weber, 1991). Thus, at elevated temperatures where the model would be significantly affected by devolatilization, the ignition temperature would perhaps be reached. Further, desiccation and devolatilization represent energy absorption phenomena that would result in actual fuel

temperatures lower than those predicted. Predictions may therefore be considered to represent an upper limit on fuel temperature.

A steady-state energy balance performed on the fuel element yields

$$q_{rad,gain} = q_{conv} + q_{rad,loss} \tag{1}$$

where $q_{rad,gain}$ is the total radiation heat transfer emitted by the plane burner and absorbed by the particle, q_{conv} is the convective energy loss due to buoyancy- or forced convection-driven flow generated around the particle, and $q_{rad,loss}$ is the total radiation emitted by the fuel particle to the surroundings. The emissivity of carbon-based woody materials is very high (Incropera et al., 2007), and is assumed here to be unity for the fuel samples studied.

The medium separating the fuel elements from the burner is assumed to be volumetrically non-participating, and therefore the burner-fuel radiation exchange is purely a surface phenomenon. Radiation transfer between the two surfaces may thus be treated using the radiation exchange factor (Siegel & Howell, 2002). Because the fuel element is much smaller than the burner, the radiation exchange factor from a finite rectangular area (burner) to a differential element (fuel) was used, with the projected area of the cylindrical fuel element employed as the area of the differential element. Using this differential element approximation, radiation exchange is accounted for between both sides of the differential fuel element and the surroundings, as well as between the front side of the fuel and burner.

In addition to radiant loss to a cooler environment, the model also accounts for convective cooling of the fuel element. In treating the convection transfer, the fuel was considered to be a horizontal cylinder exposed to either natural convective cooling characteristic of quiescent air or forced convection cooling as would arise from wind motion. The convection heat transfer coefficient was determined from empirical correlations for both the buoyancy-driven (Churchill & Chu, 1975; Morgan, 1975) and forced convection-driven (Churchill & Bernstein, 1977) cooling scenarios. Because the results exhibited some sensitivity to the natural convection heat transfer coefficient, in practice, the coefficient was determined from an average of the empirical correlations of Churchill & Chu and Morgan. The thermophysical properties used in conjunction with this correlation were interpolated from property tables (Incropera et al., 2007).

Under these assumptions, the energy balance of Eq. (1) becomes

$$2A_{fp}\sigma\left(T_f^4 - T_\infty^4\right) - F_{fb}A_{fp}\sigma(T_b^4 - T_\infty^4) + hA_f\left(T_f^4 - T_\infty\right) = 0 \tag{2}$$

where T_f is the temperature of the fuel, A_{fp} is the projected area of the fuel, F_{fb} is the radiative exchange factor from the fuel to the burner, σ is the Stefan-Boltzman constant, T_b is the temperature of the burner, h is the convection coefficient, A_f is the circumferential area of the fuel, and T_∞ is the temperature of both the ambient air and the radiative surroundings. Note that Eq. (2) is an equation for the steady-state temperature of the fuel element, and as such, it is independent of the thermophysical properties of the fuel (subject to the assumption of a radiatively black fuel).

Equation (2) is non-linear in the unknown fuel temperature, T_f. The radiation exchange factor F_{fb} depends on the burner-fuel separation distance, and the heat transfer coefficient is an implicit function of the fuel temperature through properties evaluated at the film temperature $(T_f + T_\infty)/2$. The imposed temperature of the

rectangular plane burner (T_b) was determined by calculating the blackbody temperature corresponding to the magnitude of the emissive power measured experimentally by the narrow angle radiometer using the Stefan-Boltzmann law. The fuel temperature governed by the energy balance of Eq. (2) was determined iteratively for each fuel element position. A fuel temperature was guessed and substituted into the fourth-order temperature terms in Eq. (2), and the first-order fuel temperature in the convective cooling portion of the equation was solved. The guess was then modified by systematically adjusting it a fraction of the difference between the initial guess and that solved. Convergence was declared when Eq. (2) was satisfied to within 0.01%. In practice, the fuel element was positioned far from the burner (beginning with a burner-element separation distance of 1 m). Once the solution to Eq. (2) for T_f was determined for this position, the distance between the burner and the fuel was reduced, and the converged temperature corresponding to the previous separation distance was used as the initial guess for the new position. This procedure was followed until the location nearest the burner was reached.

Model predictions are compared to the experimental data presented previously in Figure 5, where the fuel temperature rise above ambient is plotted as a function of distance from the burner for the three fuel samples investigated experimentally. Quiescent air in the laboratory environment was assumed, and buoyancy-driven cooling of the fuel was therefore imposed. The figure reveals excellent agreement between model prediction and the experimental results with regard to dependence on burner-fuel separation distance, fuel type, and fuel size. The maximum difference between predicted fuel temperature and that measured experimentally is 10 K, with the greatest difference observed for the Ponderosa pine with its irregular geometry. Fuel temperature predictions lie within three standard deviations of the experimental

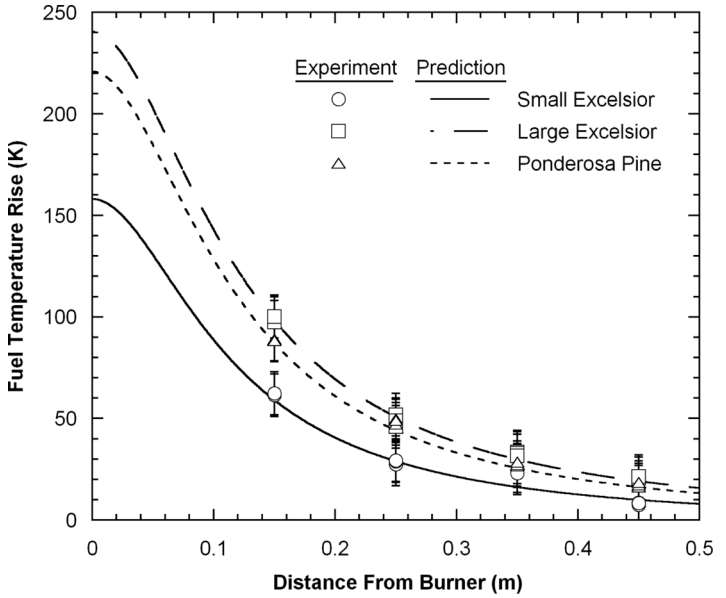

Figure 5 Comparison between model predictions and experimental measurements of fuel temperature rise.

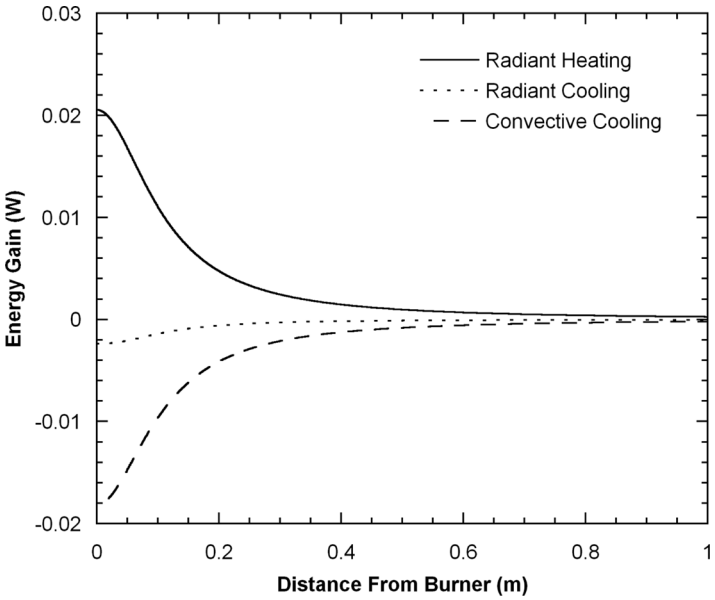

Figure 6 Predicted relative contributions of radiation heating and cooling and natural convective cooling.

measurements for all cases, and within two standard deviations for the small and large excelsior fuel samples. The excellent agreement lends confidence to the model's ability to predict the thermal response of fine fuel exposed to radiative heating.

Figure 6 illustrates the relative magnitude of fuel element heat loss/gain for a case in which the fuel diameter specified in the simulation was an average of those studied experimentally (0.8 mm), and the blackbody burner temperature imposed was calculated from an average of the experimental narrow angle radiometer measurements (890 K). It is again noted that Eq. (2) describes the steady-state temperature of the fuel and consequently is independent of fuel thermophysical properties. Of course, at steady state, the sum of all heat transfer mechanisms is identically zero at all burner-fuel element separation distances. The results of Figure 6 show that radiation gain is high near the burner and decreases as the distance between the burner and the fuel increases. The peak heat gain to the particle for these conditions is 20 mW. It is apparent that the vast majority of fuel particle cooling occurs by convection rather than radiation transfer, with radiation transfer accounting for no more than 13% of the total heat loss from the heated particle. Thus, in relative terms, the temperature of the fuel is not high enough to produce significant radiative emission, but it is high enough to generate a rather significant natural convection current around the fuel particle.

MODEL PARAMETRIC STUDY

The model developed and validated in the foregoing section was exercised to explore the effects of fuel diameter, burner size and temperature, and incident radiant flux on fuel element thermal behavior. This parametric study is undertaken both

to explore the physics of the fuel heating phenomenon, and to identify, if possible, the role of radiation heating in ignition of the fuel particles.

The fuel temperature predictive model has been validated by comparison with experimental data collected in a quiescent air environment. In an effort to better understand the range of temperatures a fuel element might experience under different convective environmental conditions, the model was extended to a forced convective cooling scenario. As stated previously, the magnitude of the forced convective cooling was determined using the empirical correlation for the heat transfer coefficient of Churchill and Bernstein (1977) for forced convection from a horizontal cylinder. This was done for wind speeds of 1, 3, and 5 m/s (11 mi/hr). Figure 7 illustrates the dependence of predicted fuel element temperature on incident radiant flux for the natural and forced convection conditions investigated. The predictions of Figure 7 are for the limiting case of an infinitely large burner (i.e., vanishing separation distance between burner and fuel element). It should be noted that experimental measurements in field burns (Frankman, 2009) reveal ground fire peak radiant heat fluxes to be between 50 and 150 kW/m^2, with flux levels in crown fires to be between 200 and 300 kW/m^2. This is confirmed by Butler et al. (2004), who report average peak heat fluxes to be 200 kW/m^2 with a maximum of 290 kW/m^2 in a crown fire. The ignition temperature line in Figure 7 indicates the minimum fuel temperature, 523 K, at which ignition may occur (Babrauskas, 2003). Thus, for a given fuel cooling condition (buoyancy- or wind-driven cooling), the incident radiant flux at which the predicted fuel temperature reaches the fuel ignition point is that flux which will result in combustion. The figure illustrates the significant difference that

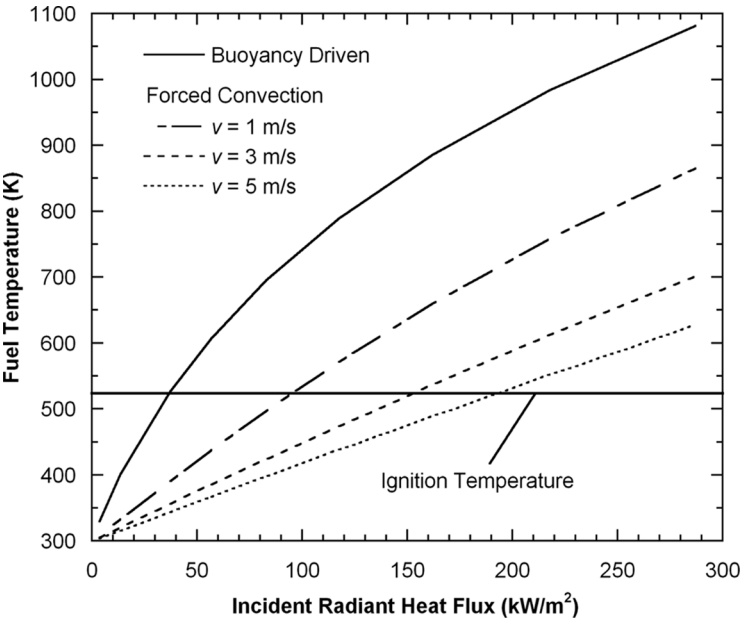

Figure 7 Predicted fuel temperature as a function of incident radiation flux for different convective conditions. The ignition temperature indicated is the minimum temperature at which wood will ignite regardless of the heating arrangement (Babrauskas, 2003).

exists between buoyancy-driven cooling and that which results from forced flow. Differences in predicted fuel temperature for the buoyancy-driven cooling and the forced flow at a wind speed of 1 m/s exceed 200 K at incident radiant fluxes above 100 kW/m^2. As expected, increases in wind speed result in lower predicted fuel temperature. Also, the figure reveals that fuel reaches the ignition temperature at lower incident radiant heat flux, as the forced convection wind speed is reduced. The limiting buoyancy-driven fuel cooling condition reveals that ignition may be reached for an incident radiant flux as low as 50 kW/m^2. It should be noted, however, that in the wildland fire environment, a quiescent condition is unlikely to prevail. Significant buoyancy-driven in-drafts are present at the flame front that draw cool ambient air into the flame front as oxygen is consumed in the combustion and high-temperature combustion products rise. The magnitude of the wind speed in such in-drafts will, of course, be a complex function of the flame environment. Field measurements by Butler (2003) suggest that air velocities of 1 to 10 m/s are common in naturally spreading crown fires with significantly higher transient gusts. Considering the potential for relatively strong in-drafts, the results of Figure 7 suggest that radiant heating alone may be insufficient to cause ignition of the fuel.

Figure 8 shows the predicted fuel temperature plotted as a function of burner (flame) temperature for burner-fuel element spacings ranging from 0 to 0.3 m. These simulations are for the limiting and perhaps unlikely case of buoyancy-driven convective cooling of the fuel element with a radiating plane burner of the size used in the experiments (0.15 m × 0.23 m). Despite their limitations, the results are illustrative of important trends. As expected, Figure 8 shows that increasing the temperature of the plane burner results in an increase in the temperature of the fuel. Also not

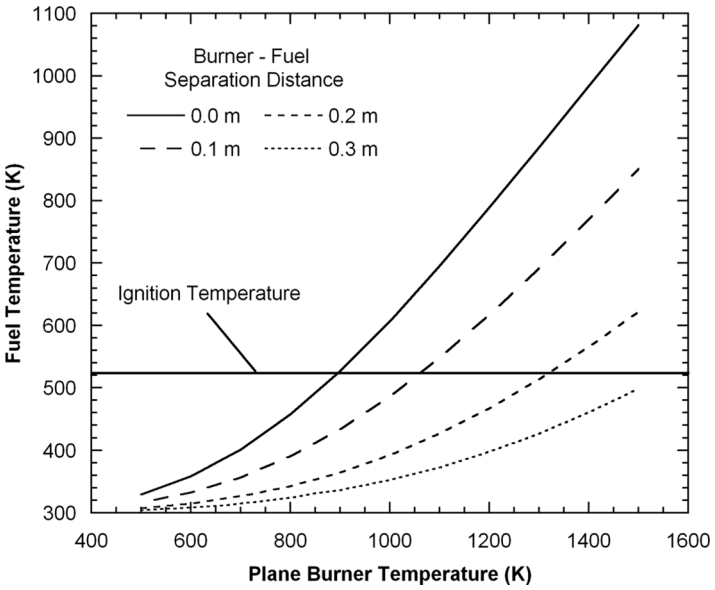

Figure 8 Sensitivity of predicted fuel temperature to plane burner temperature. The ignition temperature indicated is the minimum temperature at which wood will ignite regardless of the heating arrangement (Babrauskas, 2003).

unexpected is the fact that this increase is not as pronounced as the burner-fuel separation distance increases. For a burner of finite size, increasing separation distance between burner and fuel element results in reduced incident radiation flux on the particle. Also shown in Figure 8 is the accepted minimum fuel ignition temperature (Babrauskas, 2003). For the finite burner explored here, only fuel particles nearest the flame and subjected to irradiation from a higher temperature source are prone to reach the ignition temperature by radiant heating. In the limit of a large flame (i.e., vanishing separation distance from the burner) and for optically thick flames, the burner temperature and radiant flux incident on the fuel particle may be related through the Stefan-Boltzmann law. In this limiting and very unlikely case, the predictions reveal that a flame temperature of nominally 900 K is required for fuel ignition.

The dependence of predicted fuel temperature on fuel element diameter is illustrated in Figure 9 for a burner temperature of 890 K and natural convection cooling of the fuel element at four different burner-fuel separation distances. This burner temperature is the average of the blackbody temperatures determined from the narrow angle radiometer flux measurements in the experiments. Increasing the fuel diameter results in an increase in fuel surface temperature at all burner separation distances. Fuel surface temperature is quite sensitive to fuel diameter for very small fuel elements, more particularly near the burner. The fuel temperature is observed to be less sensitive to diameter as the diameter increases. Relative to the ignition temperature indicated in the figure, and for the conditions of the prediction, ignition due to radiant heating appears likely only for larger diameter fuel elements very near the burner surface. The predictions suggest that fuel element diameters less than 0.7 mm are unlikely to ignite due to radiant heating alone.

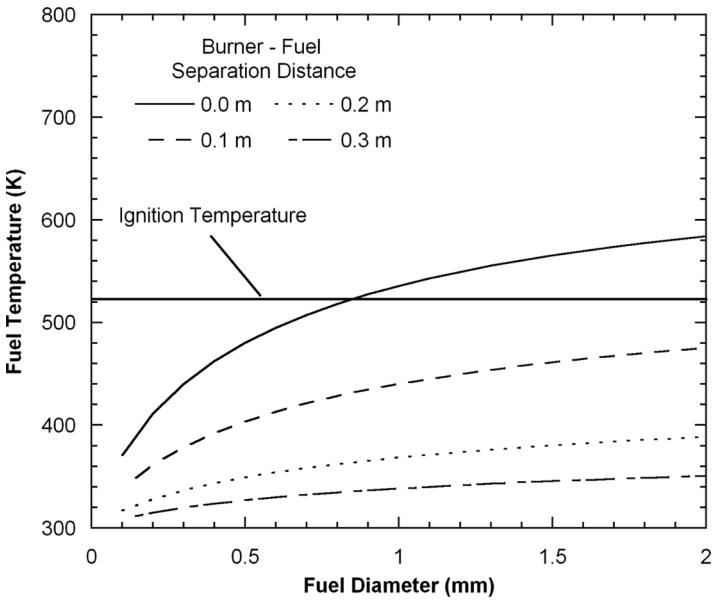

Figure 9 Dependence of predicted fuel temperature on fuel diameter. The ignition temperature indicated is the minimum temperature at which wood may ignite regardless of the heating arrangement (Babrauskas, 2003).

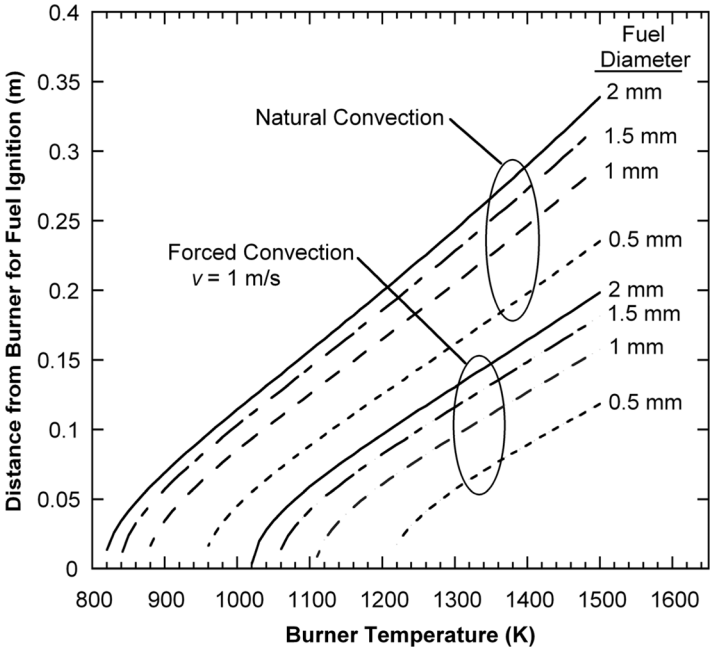

Figure 10 Predicted distance from burner at which fuel ignition (Babrauskas, 2003) may occur as a function of burner temperature.

Figure 10 shows the distance at which the fuel reaches 523 K, the minimum ignition temperature indicated by Babrauskas (2003), as a function of burner temperature for a range of fuel diameters. Both natural convection fuel cooling and forced convection cooling with a velocity of $v = 1\,\mathrm{m/s}$ are represented here. It is seen that even a moderate air velocity drastically changes the distance at which fuel may ignite by radiation only. In addition, air velocities higher than 1 m/s will ignite only at unrealistically high burner temperatures. Again, it appears that while particle ignition may occur due to radiation transfer, it is likely to occur only under the most extreme of circumstances—namely, very low ambient air velocity or very high irradiation. However, this general observation applies only to scenarios where the flame is much larger than the fuel. By way of reminder, it is emphasized that as the fuel approaches the ignition temperature, desiccation and de-volatilization (which are not included in the model) would result in energy losses and increase the energy required for particle ignition. Thus, these energy transfer mechanisms result in further reductions in temperature and strengthen the general conclusions.

CONCLUSIONS

A model has been developed to predict the steady-state temperature of fine fuels subject to irradiation from a burner of known size and temperature. The model was validated by comparison with experimental data gathered for poplar excelsior of two sizes and Ponderosa pine needles. The model presented here accurately predicts the heat transfer of fine fuels with an incident radiant flux cooled by radiant emission

and natural convection. Parametric studies suggest that ignition of the fuel element by radiation heating alone is likely only under circumstances where the fire is very intense (such as crown fires) and even then may still be dependent on pilot ignition sources.

REFERENCES

Albini, F.A. 1985. A model for fire spread in wildland fuels by radiation. *Combust. Sci. Technol.*, **42**(5&6), 229.

Albini, F.A. 1986. Wildland fire spread by radiation—a model including fuel cooling by natural convection. *Combust. Sci. Technol.*, **45**, 101.

Anderson, H.E. 1969. *Heat Transfer and Fire Spread*, Intermountain Forest and Range Experiment Station, Forest Service, U.S. Department of Agriculture, Ogden, Utah.

Asensio, M.I., and Ferragut, L. 2002. On a wildland fire model with radiation. *Int. J. Numer. Methods Eng.*, **54**, 137.

Babrauskas, V. 2003. *Ignition Handbook*, Fire Science Publishers, Issaquah, Wash.

Butler, B.W. 1993. Experimental measurements of radiant heat fluxes from simulated wildfire flames. *12th International Conference on Fire and Forest Meteorology*, Society of American Foresters, October 26–28, Jekyll Island, Ga.

Butler, B.W. 2003. Field measurements of radiant energy transfer in full scale wind driven crown fires. *6th ASME-JSME Thermal Engineering Conference*, Japan Society of Mechanical Engineers, March 16–20, Hawaii.

Butler, B.W., Cohen, J., Latham, D.J., Schuette, R.D., Sopko, P., Shannon, K.S., Jimenez, D., and Bradshaw, L.S. 2004. Measurements of radiant emissive power and temperatures in crown fires. *Can. J. For. Res.*, **34**, 1577.

Catchpole, W.R., Catchpole, E.A., Butler, B.W., Rothermel, R.C., Morris, G.A., and Latham, D.J. 1998. Rate of spread of free-burning fires in woody fuels in a wind tunnel. *Combust. Sci. Technol.*, **131**, 1.

Churchill, S.W., and Bernstein, M. 1977. Correlating equation for forced convection from gases and liquids to a circular cylinder in crossflow. *J. Heat Transfer*, **99**, 300.

Churchill, S.W., and Chu, H.S. 1975. Correlating equations for laminar and turbulent free convection from a horizontal cylinder. *Int. J. Heat Mass Transfer*, **18**, 1049.

Drysdale, D.D. 1985. *An Introduction to Fire Dynamics*, John Wiley and Sons, New York.

Dupuy, J.L. 2000. Testing two radiative physical models for fire spread through porous forest fuel beds. *Combust. Sci. Technol.*, **155**, 149.

Frankman, D. 2009. Radiation and convection heat transfer in wildland fire environments. Ph.D. Dissertation, Department of Mechanical Engineering, Brigham Young University, Provo, Utah.

Hirano, T., and Sato, K. 1974. Effect of radiation and convection on gas velocity and temperature profiles of flames spreading over paper. *15th Symp. (Int.) Combust.*, The Combustion Institute, Pittsburgh, Pa.

Incropera, F.P., Dewitt, D.P., Bergman, T.L., and Lavine, A.S. 2007. *Fundamentals of Heat and Mass Transfer*, 6th ed., John Wiley & Sons, New York.

Konev, E.V., and Sukhinin, A.I. 1977. The analysis of flame spread through forest fuel. *Combust. Flame*, **28**, 217.

Morgan, V.T. 1975. The overall convective heat transfer from smooth circular cylinders. In Irvine, T.F. and Harnett, J.P. (Eds.) *Advances in Heat Transfer*, Academic Press, New York, Vol. 11, pp. 199–264.

Munson, B.R., Young, D.F., and Okiishi, T.H. 2002. *Fundamentals of Fluid Mechanics*, 4th ed., John Wiley & Sons, New York.

Ostrach, S. 1953. An analysis of laminar free-convection flow and heat transfer about a flat plate parallel to the direction of the generating body force. *NACA Report*, 1111.

Pagni, P.J. 1972. Flame spread through porous fuels. *14th Symp. (Int.) Combust.*, The Combustion Institute, Pittsburgh, Pa.

Shaddix, C.R. 1998. Practical aspects of correcting thermocouple measurements for radiation loss. *1998 Fall Meeting of the Western States Section*, The Combustion Institute, University of Washington, March 23–24, Seattle, Wash.

Siegel, R., and Howell, J.R. 2002. *Thermal Radiation Heat Transfer*, 4th ed., Taylor and Francis, New York.

Simms, D.L. 1963. On the pilot ignition of wood by radiation. *Combust. Flame*, **7**, 253.

Stamm, A.J. 1964. *Wood and Cellulose Science*, Ronald Press Co., New York.

Susott, R.A. 1980. Thermal behavior of conifer needle extractives. *For. Sci.*, **26**, 347.

Telisin, H.P. 1973. Flame radiation as a mechanism of fire spread in forests. In Afgan, N.H. and Beer, J.M. (Eds.) *Heat Transfer in Flames*, John Wiley, New York, Toronto, London, pp. 441–449.

Van Wagner, C.E. 1967. Calculations on forest fire spread by flame radiation. *Special Paper for the 6th World Forestry Conference*, Can. Dept. For. Rep. No. 1185, Madrid, Spain.

Weber, R.O. 1991. Modeling fire spread through fuel beds. *Prog. Energy Combust. Sci.*, **17**, 67.

Wykoff, W.R. 2002. Measuring and modeling surface area of ponderosa pine needles. *Can. J. For. Res.*, **32**, 1.